the plant journal

SEB Society for Experimental Biology

The Plant Journal (2016) **85,** 107–119 doi: 10.1111/tpj.13094

Tomato fruit carotenoid biosynthesis is adjusted to actual ripening progression by a light-dependent mechanism

Briardo Llorente[1,*], Lucio D'Andrea[1], M. Aguila Ruiz-Sola[1,†], Esther Botterweg[1,‡], Pablo Pulido[1,‡], Jordi Andilla[2], Pablo Loza-Alvarez[2] and Manuel Rodriguez-Concepcion[1,*]

[1]Centre for Research in Agricultural Genomics, (CRAG) CSIC-IRTA-UAB-UB, Campus UAB Bellaterra, 08193 Cerdanyola del Valles (Barcelona), Spain, and

[2]Institut de Ciencies Fotoniques (ICFO), Barcelona Institute of Science and Technology, 08860 Castelldefels (Barcelona), Spain

Received 27 October 2015; accepted 23 November 2015; published online 9 December 2015.

*For correspondence (e-mails briardo.llorente@cragenomica.es; manuel.rodriguez@cragenomica.es).

†Present address: Department of Biology, ETH Zürich, Universitätsstraße 2, 8092 Zürich, Switzerland.

‡Present address: Copenhagen Plant Science Centre, Department of Plant and Enviromental Sciences, University of Copenhagen, Frederiksberg C, Copenhagen, Denmark.

SUMMARY

Carotenoids are isoprenoid compounds that are essential for plants to protect the photosynthetic apparatus against excess light. They also function as health-promoting natural pigments that provide colors to ripe fruit, promoting seed dispersal by animals. Work in *Arabidopsis thaliana* unveiled that transcription factors of the phytochrome-interacting factor (PIF) family regulate carotenoid gene expression in response to environmental signals (i.e. light and temperature), including those created when sunlight reflects from or passes though nearby vegetation or canopy (referred to as shade). Here we show that PIFs use a virtually identical mechanism to modulate carotenoid biosynthesis during fruit ripening in tomato (*Solanum lycopersicum*). However, instead of integrating environmental information, PIF-mediated signaling pathways appear to fulfill a completely new function in the fruit. As tomatoes ripen, they turn from green to red due to chlorophyll breakdown and carotenoid accumulation. When sunlight passes through the flesh of green fruit, a self-shading effect within the tissue maintains high levels of PIFs that directly repress the master gene of the fruit carotenoid pathway, preventing undue production of carotenoids. This effect is attenuated as chlorophyll degrades, causing degradation of PIF proteins and boosting carotenoid biosynthesis as ripening progresses. Thus, shade signaling components may have been co-opted in tomato fruit to provide information on the actual stage of ripening (based on the pigment profile of the fruit at each moment) and thus finely coordinate fruit color change. We show how this mechanism may be manipulated to obtain carotenoid-enriched fruits.

Keywords: carotenoid, fruit, ripening, shade, tomato, phytochrome-interacting factor.

INTRODUCTION

Fleshy fruits typically lose their green color during ripening and accumulate pigments that provide a distinctive color to the ripe fruit. It is assumed that these pigment changes evolved as an adaptive characteristic that attracts seed-dispersing animals once seeds have matured and are therefore able to germinate (Klee and Giovannoni, 2011; Seymour *et al.*, 2013; Zhong *et al.*, 2013). Of the three major groups of plant pigments other than chlorophylls (anthocyanins, betalains and carotenoids), only carotenoids are essential for plant life as photoprotectants of the photosynthetic apparatus against excess light and as hormone precursors (Fraser and Bramley, 2004; Ruiz-Sola and Rodriguez-Concepcion, 2012). In tomato (*Solanum lycopersicum*), a leading vegetable crop and the main model system for fleshy fruits, enhanced production of carotenoids contributes to visual changes in color during ripening. Thus, the green color of mature (full-sized) tomato fruits changes to orange and red when ripe due to breakdown of chlorophylls and accumulation of the orange carotenoid β–carotene and the red carotenoid lycopene in the fruit flesh (i.e. the pericarp) (Tomato Genome Consortium, 2012; Fantini *et al.*, 2013; Seymour *et al.*, 2013) (Figure S1). In addition to conferring attractive colors, carotenoids increase the nutritional quality of the fruit as they serve as precursors for the production of retinoids (including vitamin A) and provide many other health-related

benefits (Fraser and Bramley, 2004; Ruiz-Sola and Rodriguez-Concepcion, 2012).

Previous studies have shown that, in addition to endogenous developmental, hormonal and epigenetic regulation, environmental factors such as light have a profound influence on fruit ripening (Azari *et al.*, 2010). In particular, fruit-localized phytochromes have been found to control various aspects of tomato ripening, including carotenoid accumulation (Alba *et al.*, 2000; Schofield and Paliyath, 2005; Gupta *et al.*, 2014). Phytochromes are photoreceptors of red light (R; wavelength 660 nm) and far-red light (FR; wavelength 730 nm) that exist in a dynamic photoequilibrium between the inactive R-absorbing Pr form and the active FR-absorbing Pfr form (Neff *et al.*, 2000; Azari *et al.*, 2010). Low R/FR ratios shift the equilibrium to the inactive Pr form, while high R/FR ratios shift it to the active Pfr form. Work in *Arabidopsis thaliana* has shown that Pfr translocates to the nucleus upon photoactivation to interact with transcription factors of the bHLH phytochrome-interacting factor (PIF) family, causing their inactivation, mainly by proteasome-mediated degradation, and hence regulating gene expression (Bae and Choi, 2008; Leivar and Monte, 2014). Our previous results (Toledo-Ortiz *et al.*, 2010, 2014; Bou-Torrent *et al.*, 2015) demonstrated that Arabidopsis PIF1 and other members of the so-called PIF quartet (collectively referred to as PIFq) repress carotenoid biosynthesis both in the dark and in response to a reduction in the R/FR ratio, a plant proximity signal referred to as 'shade' that is generated due to the preferential absorbance of R by leaves of neighboring or canopy plants (Martínez-García *et al.*, 2010; Casal, 2013). Phytochrome-mediated degradation of PIFq proteins de-represses carotenogenesis during seedling de-etiolation under R or high R/FR ratio light (e.g. white light or direct sunlight). Specifically, PIF1 was shown to repress carotenoid biosynthesis mainly by binding to a G–box motif in the promoter of the single Arabidopsis gene encoding phytoene synthase (PSY), the first and main rate-determining enzyme of the carotenoid pathway (Fraser *et al.*, 2002; Toledo-Ortiz *et al.*, 2010; Ruiz-Sola and Rodriguez-Concepcion, 2012). The role of PIF1 as a direct negative regulator of *PSY* expression is antagonized by the bZIP transcription factor LONG HYPOCOTYL 5 (HY5). In contrast to PIFq proteins, HY5 is degraded in the dark but accumulates in the light and induces *PSY* expression upon binding to the same promoter motif bound by PIF1 (Toledo-Ortiz *et al.*, 2014). The repression/activation module formed by PIF1 and HY5 also provides robustness to the control of *PSY* expression by temperature cues (Toledo-Ortiz *et al.*, 2014). By contrast, HY5 appears not to be relevant in regulating *PSY* expression after perception of a low R/FR signal (i.e. shade) (Bou-Torrent *et al.*, 2015). PIF1 and other PIFq proteins are not required to control *PSY* gene expression in Arabidopsis roots (Ruiz-Sola *et al.*, 2014a).

Arabidopsis and tomato diverged some 100 million years ago (Ku *et al.*, 2000), and their different histories of polyploidization and subsequent gene loss have resulted in different numbers of paralogs for carotenoid biosynthesis enzymes, including PSY (Ruiz-Sola and Rodriguez-Concepcion, 2012; Tomato Genome Consortium 2012). Three genes encode PSY in tomato, but only one (*PSY1*) contributes to carotenoid biosynthesis during fruit ripening (Fray and Grierson, 1993; Giorio *et al.*, 2008; Tomato Genome Consortium 2012; Fantini *et al.*, 2013). Transcriptional induction of the *PSY1* gene actually fuels the burst in carotenoid biosynthesis that takes place at the onset of ripening (Fray and Grierson, 1993; Giorio *et al.*, 2008; Tomato Genome Consortium 2012; Fantini *et al.*, 2013). Transcription factors of the MADS box family, such as RIPENING INHIBITOR (RIN) and FRUITFULL 1 (FUL1/TDR4), which are positive regulators of ripening, were found to stimulate carotenoid biosynthesis by directly binding to the promoter of the *PSY1* gene to induce its expression (Martel *et al.*, 2011; Fujisawa *et al.*, 2013, 2014; Shima *et al.*, 2013). HY5 is also known to positively regulate carotenoid accumulation in tomato fruit (Liu *et al.*, 2004), whereas other components of light signaling pathways have been described as negative regulators of ripening and carotenoid biosynthesis (Azari *et al.*, 2010). However, the molecular pathways connecting the perception of light signals with the regulation of carotenoid gene expression remain unknown. Here we demonstrate that a tomato ripening-induced PIF1 homolog (PIF1a) directly binds to the promoter of the *PSY1* gene to repress fruit carotenoid biosynthesis, indicating that basic molecular mechanisms for the light-dependent control of carotenogenesis are conserved in Arabidopsis leaves and tomato fruits. Most strikingly, we propose that this PIF-dependent core mechanism plays a different biological function during fruit development, i.e. to continuously monitor the progression of ripening based on the perception of fruit pigment composition changes.

RESULTS

The ripening-induced tomato PIF1 homolog PIF1a is a true PIF

Phytochromes have been proposed to control PSY activity and carotenoid biosynthesis in tomato fruit (Alba *et al.*, 2000; Schofield and Paliyath, 2005; Gupta *et al.*, 2014). While the changes in *PSY1* transcript levels observed when fruits are irradiated with R or exposed to simulated shade (i.e. FR-enriched white light) support a positive role for phytochrome signaling in modulating *PSY1* gene expression (Figure S2), the precise molecular mechanism awaits investigation. Because PIF1 is directly involved in phytochrome-dependent regulation of the single Arabidopsis *PSY* gene (Toledo-Ortiz *et al.*, 2010, 2014; Bou-Torrent *et al.*, 2015), we first evaluated whether tomato PIF1 homo-

logs are present in the fruit to regulate *PSY1* expression during ripening. A survey of the tomato genome (Tomato Genome Consortium 2012) for PIF sequences found six genes, including two with homology to Arabidopsis PIF1 (Figure 1a). The tomato gene encoding the PIF-like protein most closely related to Arabidopsis PIF1 (Figure 1a) was named *PIF1a* (Solyc09 g063010). Analysis of the Tomato Functional Genomics Database (http://ted.bti.cornell.edu/) and quantitative PCR analysis of transcript levels (Figure 1b) showed that, unlike the close homolog *PIF1b* (Solyc06g008030), *PIF1a* is expressed in the fruit and induced during ripening. The level of transcripts encoding PIF1a remained virtually constant during the maturation process, i.e. when immature green fruit grow to achieve their final size at the mature green (MG) stage. However, upon induction of ripening, *PIF1a* transcript levels increased approximately twofold at the orange (OR) stage and approximately fivefold in red ripe (RR) fruit compared to MG samples (Figure 1b). We therefore selected PIF1a for further studies.

To confirm whether PIF1a functions as a PIF, we evaluated its subcellular localization (Figure 1c), its light-dependent stability (Figure 1d), and its *in vivo* activity (Figure 1e). Transient expression assays in *Nicotiana benthamiana* leaves confirmed localization of a GFP-tagged PIF1a protein (PIF1a–GFP) in nuclear bodies (Figure 1c), as expected for a true PIF transcription factor (Al–Sady *et al.*, 2006; Shen *et al.*, 2008; Trupkin *et al.*, 2014). Also as expected, the PIF1a–GFP protein was degraded when nuclei were irradiated with R (i.e. upon activation of phytochromes) but not

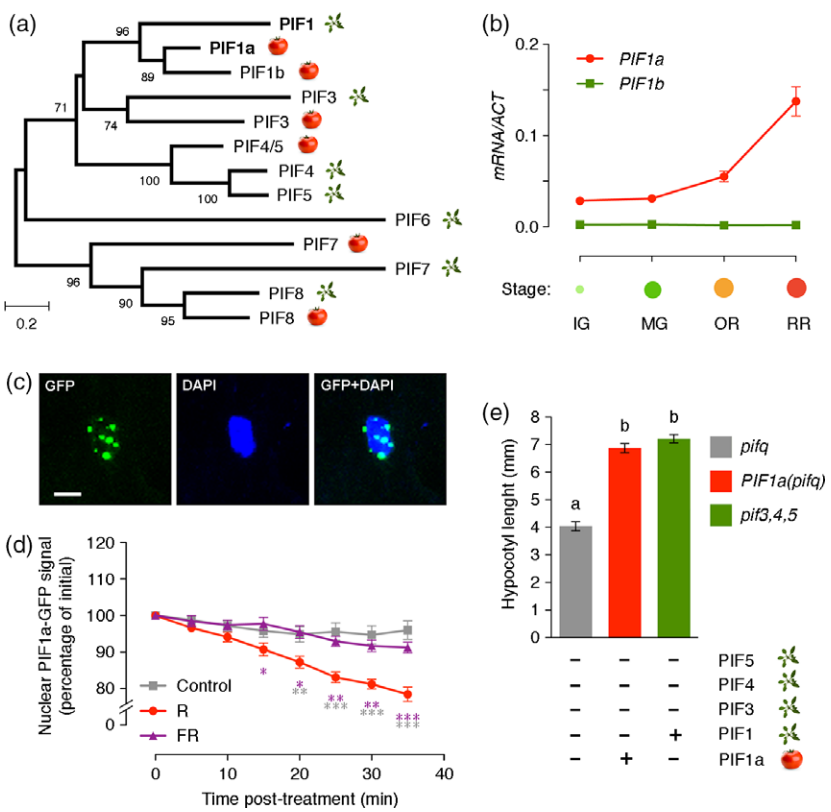

Figure 1. Tomato PIF homologs.

(a) Maximum-likelihood tree constructed using Arabidopsis and putative tomato PIF sequences. The percentage of trees in which the associated sequences clustered together with >70% reliability is shown next to the branches. The scale bar represents the mean number of substitutions per site. Images indicate the species.

(b) Quantitative PCR analysis of transcript levels for tomato PIF1 homologs during fruit ripening. IG, immature green; MG, mature green; OR, orange; RR, red ripe. Values are means ± SEM of $n \geq 5$ independent samples.

(c) Confocal microscopy images of GFP and DAPI fluorescence in the nucleus of a *N. benthamiana* leaf cell transiently expressing a GFP-tagged tomato PIF1a protein. Scale bar = 5 μm.

(d) Quantification of PIF1a–GFP fluorescence in nuclei such as those shown in (c) for samples kept in the dim light of the microscope room (control) or illuminated with supplemental R or FR light for the indicated times ($n \geq 11$). Values are means ± SEM, and significant differences (according to ANOVA followed by Newman–Keuls) compared with the symbols of corresponding color are indicated by asterisks (*$P < 0.05$, **$P < 0.01$, ***$P < 0.001$).

(e) Hypocotyl length of etiolated Arabidopsis seedlings defective in PIF1, PIF3, PIF4 and PIF5 (*pifq*) compared to triple mutants expressing wild-type PIF1 (*pif3,4,5*) and quadruple mutants expressing the tomato *PIF1a* sequence ($n = 25$). Values are means ± SEM, and significant differences (according to ANOVA followed by Newman–Keuls) are indicated by different letters ($P < 0.0001$).

when irradiated with FR or when kept under dim light (Figure 1d). As shown in Figure 1(e), expression of the tomato *PIF1a* gene under the control of the constitutive CaMV 35S promoter in an Arabidopsis quadruple mutant defective in PIF1, PIF3, PIF4 and PIF5 (*pifq*) resulted in a phenotype identical to that of the triple mutant lacking PIF3, PIF4 and PIF5 (Leivar *et al.*, 2009; Shin *et al.*, 2009; Leivar and Quail, 2011). We therefore conclude that the tomato PIF1a protein complements the loss of Arabidopsis PIF1 activity, and hence that it functions as a true PIF *in vivo*.

PIF1a represses *PSY1* expression by binding to a PBE box in its promoter

We next explored the putative role of PIF1a in the control of tomato *PSY1* expression and fruit carotenoid biosynthesis during ripening (Figure 2). Transient over-expression of the PIF1a–GFP protein in tomato pericarp tissue by agroinjection of MG fruit resulted in the eventual development of carotenoid-lacking sections as the fruit reached the RR stage (Figure 2a). This phenotype is consistent with a loss of PSY1 activity in these sections, which phenocopied the PSY1-defective mutant *yellow flesh* (*r*) (Fray and Grierson, 1993). To confirm whether PIF1a functions as a repressor of carotenoid biosynthesis in tomato fruit by down-regulating *PSY1* gene expression (similar to that reported for PIF1 and *PSY* in Arabidopsis), we next reduced *PIF1a* transcript levels and analyzed the concomitant changes in *PSY1* expression. Using a virus-induced gene silencing (VIGS) approach (Orzaez *et al.*, 2009; Fantini *et al.*, 2013), up-regulation of *PSY1* transcripts was indeed detected in *PIF1a*-silenced pericarp tissue compared with neighboring non-silenced tissue (Figure 2b). To further corroborate this observation, we generated stably transformed tomato plants harboring an artificial microRNA (Ossowski *et al.*, 2008) designed to specifically silence the *PIF1a* gene under the control of the 35S promoter (amiPIF1a lines). Consistent with the VIGS results, transgenic RR fruits showed increased levels of *PSY1* transcripts that inversely correlated with the extent of *PIF1a* silencing in various lines (Pearson correlation coefficient $r = -0.9725$; $P = 0.0054$) (Figure 2c). The expression of other tomato *PIF* genes in the fruit, including *PIF1b*, was found to be unaltered in these samples (Figure S3), confirming the specificity of the amiPIF1a construct. In agreement with the conclusion that higher *PSY1* transcript levels in amiPIF1a fruits resulted in increased PSY activity, metabolite profiling of transgenic OR and RR fruit showed higher amounts of phytoene, the direct product of PSY activity (Figure 2d). Also consistent with the rate-limiting role demonstrated for PSY activity by metabolic flux control analysis (Fraser *et al.*, 2002), levels of total carotenoids in amiPIF1 fruits were significantly higher than those in untransformed controls (Figure 2d).

Examination of the genomic sequence upstream of the translation start codon of *PSY1* revealed the existence of two conserved PIF-binding motifs (Toledo-Ortiz *et al.*, 2003; Zhang *et al.*, 2013): a G–box (CACGTG) and a PBE box (CACATG) (Figure 2e). Chromatin immunoprecipitation assays with tomato pericarp sections transiently over-expressing PIF1a–GFP (Figure 2a) indicated that PIF1a specifically binds to the PBE box of the *PSY1* promoter *in vivo* (Figure 2e). Based on these data, we conclude that PIF1a binds to the promoter of the *PSY1* gene to repress its expression and hence reduce PSY activity to eventually inhibit carotenoid biosynthesis.

Tomato fruit chlorophyll reduces the R/FR ratio of sunlight as it penetrates the fruit flesh

The ripening-associated accumulation of *PIF1a* transcripts (Figure 1b) may function as a mechanism to repress *PSY1* expression and hence antagonistically balance the effect of other ripening-induced transcription factors such as RIN and FUL1, which are direct activators of *PSY1* expression (Martel *et al.*, 2011; Fujisawa *et al.*, 2013, 2014; Shima *et al.*, 2013). However, we decided to explore new regulatory roles for PIF1a based on its properties as a PIF, specifically its phytochrome-mediated degradation response when the proportion of R increases (Figure 1d). It has been shown that the amount of R that passes through the pericarp of tomato fruit exposed to sunlight is much lower in green stages compared to orange/red stages, but the amount of FR changes very little (Alba *et al.*, 2000). However, the dynamics of light quality changes within the tissues of tomato fruits, and their potential biological relevance, remain unknown. To address the first point, we measured both the quantity (transmittance) and quality (R/FR ratio) of artificial white light (W) at increasing depths in the tomato pericarp (Figure 3 and Figure S4). Whereas transmittance showed a similar decrease in MG and OR fruit, the R/FR ratio only decreased in MG fruit. We tentatively conclude that the preferential absorbance of R (but not FR) by the chlorophyll present in fruit pericarp chloroplasts may be responsible for the observed decrease in the R/FR ratio within the cells of MG fruit, whereas this ratio was virtually unaffected by the presence of increasing amounts of carotenoids in OR fruit.

To next confirm whether the pigment composition of the fruit was responsible for the observed changes, we set up an experimental system to mimic the natural filter provided by these pigments. Total pigments were extracted from MG, OR and RR fruit, and used to characterize their chlorophyll and carotenoid composition (Figure S1) and absorbance spectra (Figure 4a). Pigment extracts from MG fruit showed an absorbance profile almost identical to that observed in leaves, with a characteristic peak at 660 nm due to the presence of chlorophylls. By contrast, this peak is almost completely absent in extracts from OR and RR fruits (Figure 4a). As a consequence, sunlight or artificial white (W) light passing

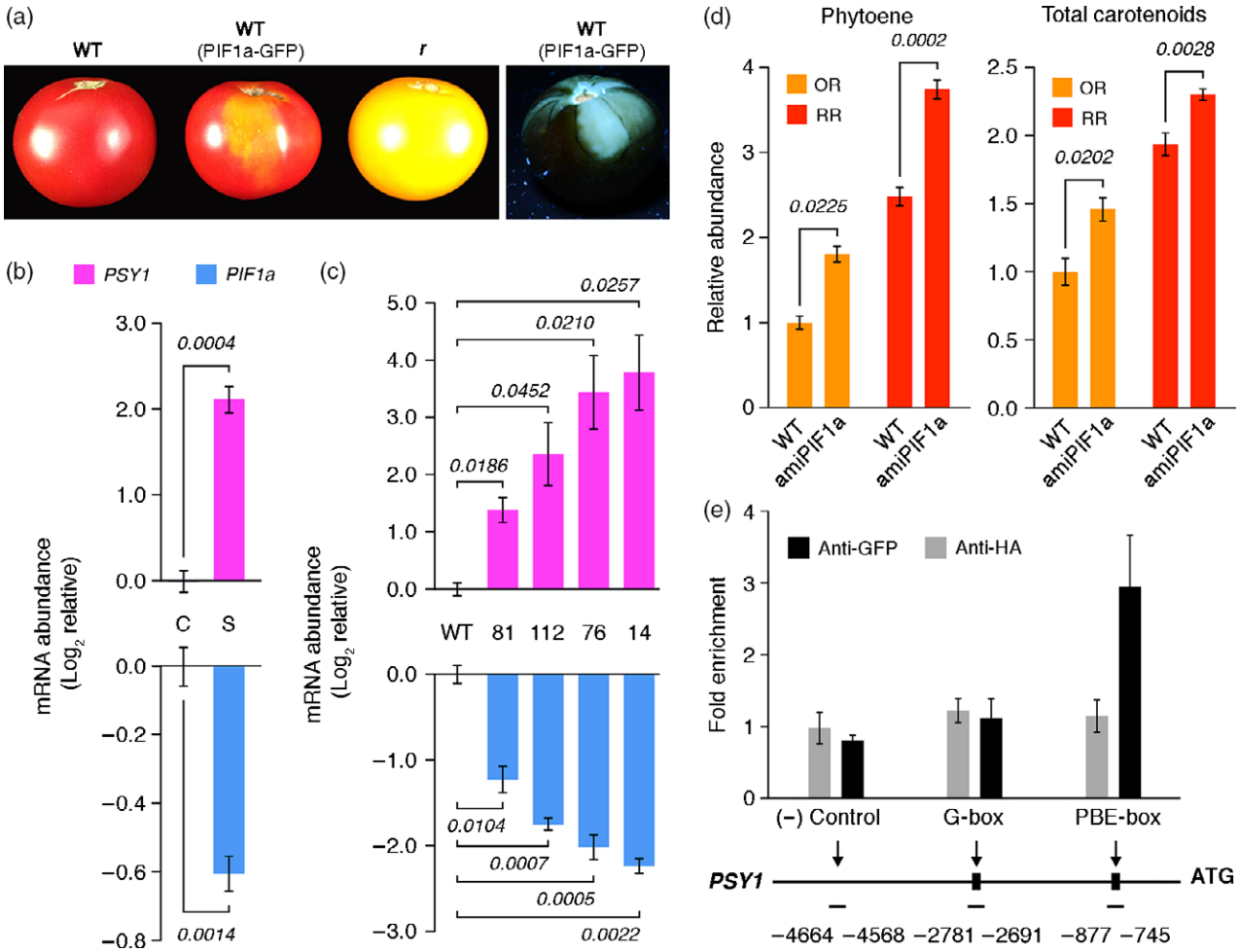

Figure 2. PIF1a directly represses *PSY1* expression in tomato fruit.
(a) Transient over-production of PIF1a in tomato fruits. Wild-type (WT) fruits at the MG stage were agroinjected with a construct to over-express the PIF1a–GFP protein, and left attached to the plant until they reached the RR stage. The fruit sections where the PIF1a–GFP protein was present (as deduced from GFP fluorescence detected by illumination with UV light, as shown on the right) showed a reduced accumulation of carotenoids, resulting in a yellow color (due to flavonoids) identical to that observed in ripe fruit of the PSY1-defective mutant *yellow ripe* (*r*).
(b) Quantitative PCR data show that VIGS-mediated down-regulation of *PIF1a* transcripts in silenced (S) sectors of tomato fruit causes an up-regulation of *PSY1* transcripts compared to non-silenced (C) sectors of the same fruits.
(c) Constitutive silencing of *PIF1a* in fruit from various transgenic tomato lines expressing a specific artificial microRNA (amiPIF1a) leads to a concomitant induction in *PSY1* transcript levels compared to untransformed (WT) controls.
(d) HPLC analysis of carotenoid levels in transgenic amiPIF1a fruits (line 112) shows an increased accumulation of phytoene (the direct product of PSY activity) and total carotenoids relative to untransformed (WT) controls at both OR and RR stages.
(e) ChIP/quantitative PCR analysis performed using tomato fruit sections transiently expressing the PIF1a–GFP protein using anti-GFP antibodies. Control reactions were processed in parallel using anti-HA serum or no antibodies. The location of *PSY1* promoter amplicons used in quantitative PCR quantification of ChIP-enriched DNA regions corresponding to control (–) and PIF-binding domains (G–box and PBE box) are indicated in the map.
Values in (b)–(d) are means ± SEM ($n \geq 3$). Italic numbers above the bars indicate *P* values (Student's *t* test). Values in (e) are means ± SEM from two independent experiments. Values are reported relative to non-silenced sectors (b), WT (c), OR (d) or blank samples (e).

through extracts from OR or RR fruit maintained a high R/FR ratio whereas the light passing through extracts from MG fruit showed a low R/FR ratio (Figure 4b and Figure S5). Almost identical results were obtained when whole hand-cut sections of pericarp tissue were used instead of extracts (Figure S5), confirming that the observed effects on light quality were due to the presence of photosynthetic pigments (chlorophylls and carotenoids) in the samples.

Fruit pigmentation-dependent changes in the R/FR ratio specifically influence *PSY1* expression

Once we had established that the pigment composition of MG fruit resulted in a reduction in the R/FR ratio of the light reaching the inner layers of pericarp cells, but the pigment composition of OR or RR fruit (rich in carotenoids but almost completely lacking chlorophylls) had little or no effect on this ratio, we assessed whether this has

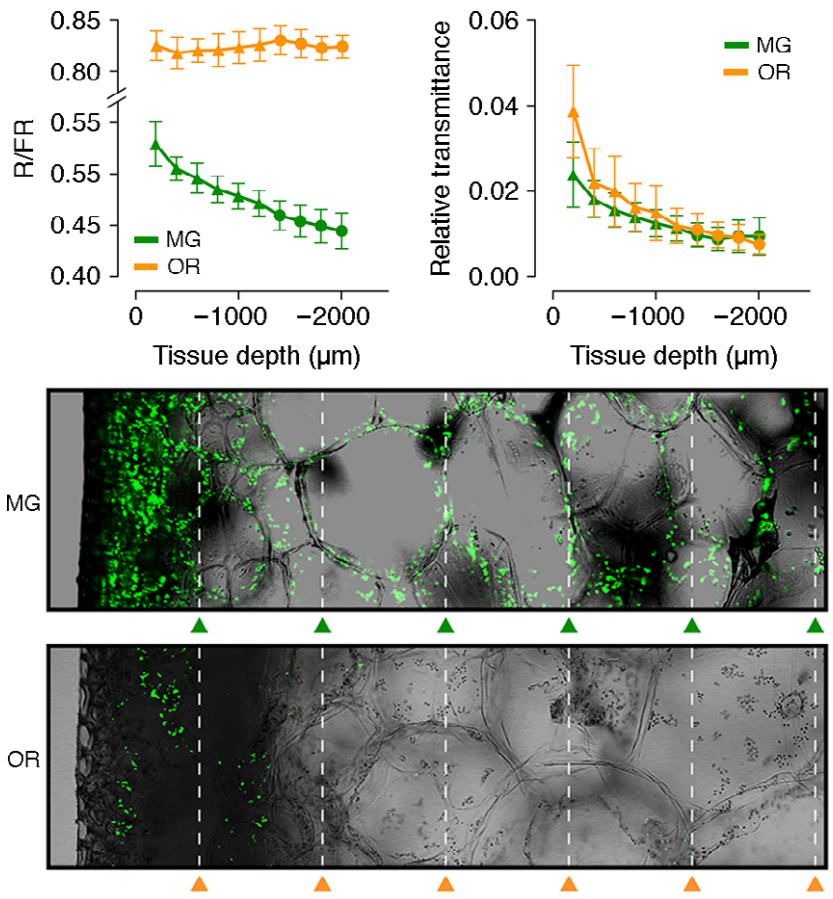

Figure 3. The R/FR ratio inside the fruit pericarp changes during ripening.
Serial sections of the outer pericarp of MG and OR fruit were obtained using a vibratome. Starting with 2000 μm thick samples, 200 μm layers were sequentially removed from the internal side of the pericarp to obtain samples of decreasing thickness until only a thin section of the fruit surface was left. After removing each 200 μm layer, the remaining section was illuminated with artificial white light, and both the R/FR ratio and the intensity (transmittance) of the light that passed through it were determined. Bright-field images of MG and OR fruit pericarp tissue merged with chlorophyll autofluorescence (corresponding to chloroplasts, green) are also shown. Dashed lines indicate the depths at which the last six light measurements were performed (represented by the triangles in the graphs). Values are means ± SEM (n = 3) relative to blank controls.

biological relevance. We designed a filter system that involved placing a glass plate containing MG and RR fruit pigment extracts between the source of light (W) and the experimental samples (Figure S6). To test whether the change in the R/FR ratio obtained after filtering of light through MG or RR filters affected gene expression, we used Arabidopsis as a well-known model for the molecular response to low R/FR signals (i.e. shade). W-grown Arabidopsis seedlings were exposed to W filtered through MG or RR filters, and the expression of known shade-regulated genes was analyzed. As shown in Figure S7, transcripts of shade-induced genes accumulated at higher levels in samples exposed to W+MG. By contrast, *PSY* expression was lower in samples illuminated with W+MG (Figure 4c), consistent with the reported down-regulation of the gene in response to shade (Bou-Torrent *et al.*, 2015). Altogether, these results demonstrate that the fruit pigments effectively alter the quality of the light that penetrates the tomato pericarp, generating signals that eventually modulate the expression of shade-responsive genes.

To confirm whether fruit pigment composition also has an effect on the regulation of tomato carotenoid biosynthetic genes, we used pigment-lacking (white) tomato fruits obtained by preventing exposure to light from the very early stages of fruit set and development (Cheung *et al.*, 1993). To avoid developmental variability among visually similar fruits, we compared the effects of illuminating the same fruit with either W+MG or W+RR. To do so, individual white fruits were longitudinally cut into two halves in the dark, and each of the halves was then treated with the corresponding light for 2 h (Figure 4d). Expression analysis of genes encoding enzymes of the carotenoid biosynthesis pathway, including *DXS1*, *PSY1*, *PSY2*, *PSY3*, *PDS*, *LCY–E*, *LCY–B* and *CYC–B* (Figure 4e), revealed that only *PSY1* exhibited significant changes, showing levels that were approximately twofold higher in the halves placed under the RR filter compared to those illuminated with W+MG (Figure 4f). Higher levels of *PSY1* transcripts in samples exposed to light with a higher R/FR ratio were expected as a consequence of the instability of the PIF1a repressor under such conditions (Figure 1d).

Changes in the R/FR ratio of the light sensed in pericarp cells probably adjust carotenoid biosynthesis to the actual progress of ripening

We next tested whether the differential light-filtering properties of fruit pigments also affect carotenoid metabolism during fruit ripening (Figure 5). Because this experiment

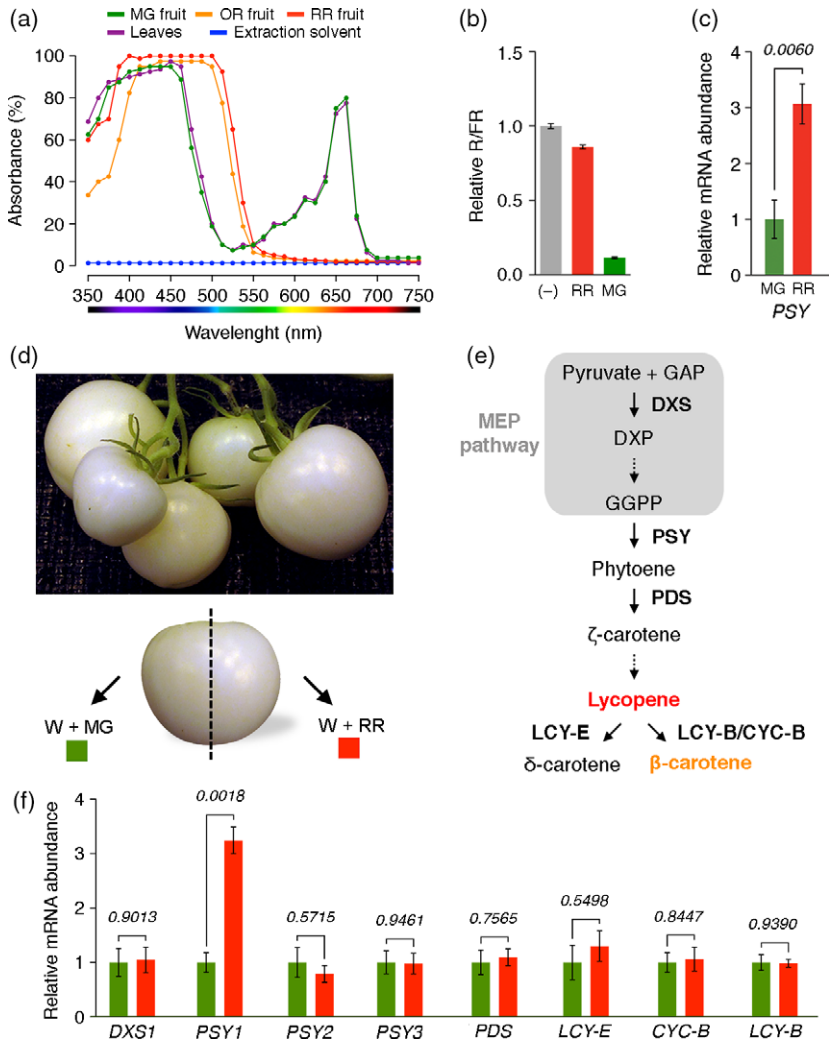

Figure 4. Light filtered through tomato fruit photosynthetic pigments specifically affects the expression of PSY-encoding genes.
(a) Absorption spectra of organic extracts of photosynthetic pigments (chlorophylls and carotenoids) isolated from tomato leaves and fruits at various developmental stages.
(b) R/FR ratio of artificial white light (W) filtered through pigment extracts prepared from red (RR) or green (MG) fruits relative to that of unfiltered light (–). Values are means ± SEM ($n \geq 6$).
(c) Effect of light filtered through tomato MG or RR extracts on expression of the Arabidopsis *PSY* gene. Arabidopsis seedlings germinated and grown in the dark for 3 days were exposed for 1 h to W filtered through MG or RR filters. Transcript abundance was assessed by quantitative PCR, Values are means ± SEM ($n = 4$) relative to the MG filter condition. The number above the bars indicates the *P* value (Student's *t* test).
(d) Tomato fruits lacking any kind of endogenous pigments were obtained approximately 40 days after covering whole inflorescences with light-proof bags. The resulting white fruits were collected in the bags and then cut in two halves in the dark. Each of the halves was immediately exposed for 2 h to W light filtered through MG or RR filters.
(e) Enzymes of the carotenoid biosynthesis pathway in tomato. The methylerythritol 4–phosphate (MEP) pathway provides substrates for the carotenoid pathway, while PSY leads to downstream accumulation of carotenoids. GAP, glyceraldehyde-3–phosphate; DXP, deoxyxylulose-5–phosphate; GGPP, geranylgeranyl diphosphate. Solid and dashed arrows represent single or multiple enzymatic steps, respectively. Enzymes are shown in bold: DXS, DXP synthase; PSY, phytoene synthase; PDS, phytoene desaturase; LCY–E, lycopene ε–cyclase; LCY–B, lycopene β–cyclase; CYC–B, chromoplast-specific lycopene β–cyclase.
(f) Quantitative PCR analysis of samples treated as described in (d) to estimate the abundance of transcripts for tomato genes encoding the enzymes indicated in (e). Values are means ± SEM from $n = 3$ biological replicates relative to the W+MG condition. The numbers above the bars indicate *P* values (Student's *t* test).

required irradiating fruit at a pre-ripening stage and visually identifying the developmental stage was not possible in the case of white fruit, we used MG fruit. Individual fruits were split in two halves immediately before exposing each half to either W+MG or W+RR. Exposure was maintained for a few days until both halves had entered the breaker stage (i.e. started losing chlorophylls and turning orange/red). Reaching this stage typically took longer for fruit halves illuminated with W+MG (Figure 5a). Consistent with this visual observation, W+RR-exposed halves showed a higher accumulation of the major carotenoids lycopene and β–carotene compared with their

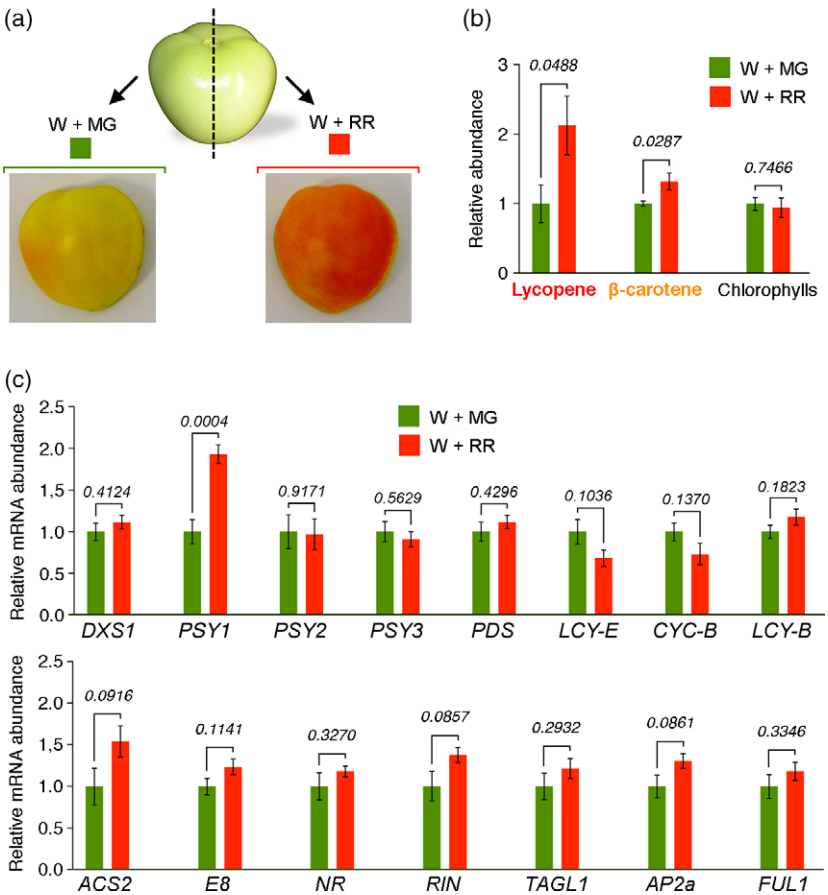

Figure 5. The light-absorbing properties of fruit photosynthetic pigments influence carotenoid biosynthesis but not ripening.
(a) Fruits at the MG stage were cut in two and exposed to W light filtered through MG or RR filters until pigmentation changes were visually observed in both halves.
(b) HPLC analysis of major photosynthetic pigments in fruit halves treated as described in (a).
(c) Quantitative PCR analysis of transcript abundance of the indicated tomato genes in fruit halves treated as described in (a). The upper graph includes genes for carotenoid biosynthetic enzymes, and the lower graph corresponds to ripening-related genes. Values are means ± SEM from $n = 6$ biological replicates relative to the W+MG condition. The numbers above the bars indicate *P* values (Student's *t* test).

W+MG-exposed counterparts, while chlorophylls were not affected by the light filters (Figure 5b). Similar to the results obtained with white fruits, the halves illuminated with W+RR also showed a significantly increased accumulation of *PSY1* transcripts, but no changes were observed in other carotenoid-related genes (Figure 5c). We also analyzed the expression of several well-characterized ripening-related genes in the same samples. We included the genes encoding RIN and FUL1/TDR4, which are positive regulators of ripening that directly induce *PSY1* expression (Martel *et al.*, 2011; Fujisawa *et al.*, 2013, 2014; Shima *et al.*, 2013). Notably, no statistical differences were found between halves exposed to W+MG or W+RR filters (Figure 5c), suggesting that the light treatments did not have a significant influence on ripening but specifically affected fruit carotenoid biosynthesis by modulating *PSY1* expression.

In agreement with the conclusion that the R/FR ratio of the light reaching the pericarp cells affects carotenoid biosynthesis by specifically modulating *PSY1* gene expression, breaker fruits showed higher levels of *PSY1* transcripts and derived carotenoids such as phytoene (the immediate PSY product) and lycopene in the outer side of the pericarp tissue (Figure 6a), which experiences a higher R/FR ratio than the internal section (Figure 3). Furthermore, PIF1a appears to be the main factor regulating *PSY1* expression in response to this signal, as the difference in *PSY1* transcript levels observed in fruit halves exposed to W+MG or W+RR (Figure 5) is strongly attenuated in transgenic amiPIF1a fruits (Figure 6b). These results confirm that the low R/FR ratio of the light reaching the inner pericarp cells of MG fruit due to the presence of chlorophylls (referred to as a self-shading effect) represses carotenoid biosynthesis by specifically down-regulating *PSY1* gene expression via PIF1a. This effect progressively decreases as soon as chlorophylls start to disappear at the onset of ripening, thus boosting (i.e. de-repressing) *PSY1* expression and carotenoid accumulation in breaker fruits.

DISCUSSION

Carotenoids are lipophilic isoprenoid pigments that are synthesized by all photosynthetic organisms, including plants. Because they are essential to protect the photosynthetic apparatus against excess light, it is not surprising that their production is tightly regulated by light (Fraser and Bramley, 2004; Azari *et al.*, 2010; Ruiz-Sola and Rodriguez-Concepcion, 2012). Carotenoids also provide colors to fruits as a signal of ripeness, so that animals disperse the

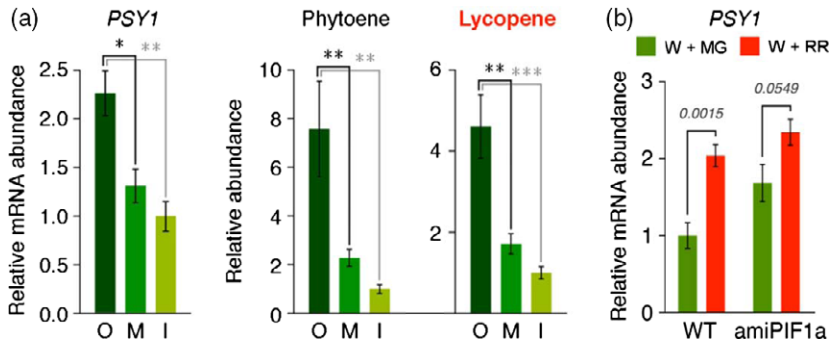

Figure 6. PIF1a regulates *PSY1* expression in response to changes in R/FR ratio.
(a) *PSY1* expression and carotenoid levels in various regions of the pericarp. The graphs represent quantitative PCR analysis of *PSY1* transcript levels and HPLC analysis of phytoene and lycopene accumulation in the outer section, i.e. that most exposed to sunlight (O), the middle section (M) and the inner section (I) (approximately 1 mm) of the pericarp of fruits at the breaker stage ($n \geq 5$). Values are means ± SEM relative to inner pericarp samples. Significant differences (according to ANOVA followed by Newman–Keuls) are indicated by asterisks (*$P < 0.05$, **$P < 0.01$, ***$P < 0.001$).
(b) Quantitative PCR analysis of *PSY1* transcript abundance in untransformed (WT) and transgenic amiPIF1a fruit halves treated as described in Figure 5(a). Values are means ± SEM from $n = 5$ biological replicates relative to the W+MG condition. The numbers above the bars indicate *P* values (Student's *t* test).

enclosed seeds only when their development has been completed. Thus, carotenoids give yellow color to bananas, orange color to peaches and oranges, and red color to tomatoes. Here we show that carotenoid biosynthesis in ripening tomato fruit is regulated by a PIF-based molecular mechanism that is identical to that regulating carotenogenesis in Arabidopsis leaves in response to light signals. A striking difference, however, is that this mechanism appears to fulfill a completely different function in tomato fruit, as it uses shade signaling components not to gather environmental information (e.g. the presence of plant neighbors that may eventually compete for resources) but to provide information on the progression of ripening based on the pigment profile of the fruit at any given moment. A model summarizing the proposed mechanism is presented in Figure 7. A self-shading effect due to the presence of high chlorophyll levels and low carotenoid levels in green fruit alters the spectral composition of the light that penetrates the pericarp (Figure 3), maintaining a relatively high proportion of phytochromes in their inactive Pr form. In this context, PIF1a accumulates (Figure 1), repressing *PSY1* gene expression by directly binding to its promoter (Figure 2). When the ripening developmental program starts, chlorophylls begin to degrade, progressively reducing the self-shading effect and consequently shifting the photoequilibrium of phytochromes to their active Pfr form. This promotes PIF1a degradation, resulting in *PSY1* de-repression and a subsequent increase in carotenoid biosynthesis (Figure 7).

It is striking that the described self-shade signaling pathway specifically targets *PSY1*, the main gene controlling the metabolic flux into the carotenoid pathway during tomato ripening (Figures 4 and 5). These findings parallel those previously described in Arabidopsis, where PIF1 specifically targets the *PSY* gene for control of carotenoid biosynthesis during de-etiolation (Toledo-Ortiz *et al.*,

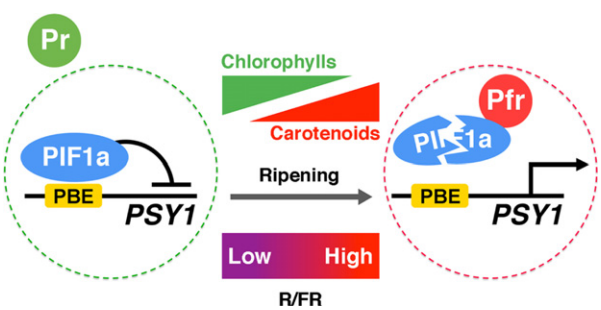

Figure 7. Self-shading model of carotenoid biosynthesis control.
Chlorophylls in green fruit generate a self-shading effect that maintains phytochromes predominantly in the inactive Pr form and high PIF1a levels that repress *PSY1* expression. Chlorophyll breakdown at the onset of ripening reduces the self-shading effect, shifting phytochromes to the active Pfr form and promoting PIF1a degradation. Consequently, *PSY1* is de-repressed and carotenoid biosynthesis is boosted. The dashed circles represent nuclei.

2010). It remains unknown whether the same mechanism is also active in tomato leaves or de-etiolating seedlings (probably involving other PIF homologs and PSY-encoding genes, as PIF1a and PSY1 appear to be mostly restricted to the fruit). While it is likely that direct transcriptional control of genes encoding PSY by PIF transcription factors may be a conserved mechanism in nature for light-mediated regulation of the carotenoid pathway, PIFs are not required to regulate *PSY* expression in Arabidopsis roots either under normal conditions or in response to abscisic acid or salt signals that promote root-specific up-regulation of the gene (Ruiz-Sola *et al.*, 2014a,b). These results suggest that PIFs may only be relevant for the control of *PSY* gene expression and carotenoid biosynthesis in organs that are normally exposed to light.

Similar to the general mechanisms involved in PIF-mediated control of carotenoid biosynthesis in Arabidopsis shoot tissues, tomato PIF1a may be part of an antagonistic

module to regulate expression of the *PSY1* gene in tomato fruit. Thus, the levels of transcripts encoding direct negative regulators of the gene such as PIF1a (Figure 1b) but also direct positive regulators such as RIN and FUL1 (Martel *et al.*, 2011; Fujisawa *et al.*, 2013, 2014; Shima *et al.*, 2013) increase during ripening. This may function as a 'gas-and-brake' mechanism to provide a more robust control of tomato *PSY1* expression during ripening, similar to that proposed to regulate Arabidopsis *PSY* expression and carotenoid biosynthesis in response to light and temperature cues (Toledo-Ortiz *et al.*, 2014; Bou-Torrent *et al.*, 2015). However, we speculate that the main function of PIF1a during ripening is to modulate the developmental control of *PSY1* expression and hence carotenoid biosynthesis by finely adjusting the transcription rate of the gene to the actual progression of ripening (Figure 7). Based on the described data, we propose that the developmental induction of *PSY1* expression directly mediated by general ripening activators such as RIN is additionally promoted by reduced PIF1a activity when chlorophylls degrade at the onset of ripening (due to the pigmentation-derived increase in the R/FR ratio). However, as ripening progresses, increasing levels of *PIF1a* transcripts may produce more protein as a buffering mechanism to counterbalance the positive effects of transcriptional activators on *PSY1* expression.

Based on the widespread occurrence of ripening-associated fruit pigmentation changes as an adaptive characteristic for attracting animals that disperse viable seeds, we propose that similar PIF-mediated mechanisms may operate in other plant species bearing fleshy fruits that lose their green color and accumulate carotenoids when ripe. Furthermore, the pigmentation-based dynamic regulation unveiled here may have implications that go beyond evolution and ecology to affect fruit biotechnology. Thus, constitutive down-regulation of PIF levels in tomato plants was shown here to be effective at increasing accumulation of carotenoids in the fruit (Figure 2d). It is predicted that more targeted manipulations of PIF levels (i.e. using fruit-specific and ripening-induced promoters) may further improve the carotenoid profile of tomato and a number of other fruits, and hence lead to successful creation of healthier, carotenoid-rich foods.

EXPERIMENTAL PROCEDURES

Plant material and growth conditions

Tomato (*Solanum lycopersicum*) and tobacco (*Nicothiana benthamiana*) plants were grown under standard greenhouse conditions (14 h light at 27 ± 1°C and 10 h dark at 22 ± 1°C). The tomato varieties MicroTom and Moneymaker were used for most experiments. White tomatoes were obtained from Moneymaker plants as described previously (Cheung *et al.*, 1993). VIGS experiments were performed using a Del/Ros1 line N in the Moneymaker background (Orzaez *et al.*, 2009). All *Arabidopsis thaliana* lines used in this work were in the Col–0 background. Arabidopsis seeds were surface-sterilized and sown on sterile Murashige and Skoog medium containing 1% agar and no sucrose. Seeds were stratified for 3 days at 4°C before use. Hypocotyl length was quantified using ImageJ (http://rsb.info.nih.gov/) as described previously (Sorin *et al.*, 2009).

Unless otherwise stated, light-filtering experiments with fruit pigment filters were performed in climate-controlled growth chambers equipped with fluorescent tubes providing continuous white light (22°C; 90 μmol m^{-2} sec^{-1} PAR). Fluence rates were measured using a SpectroSense2 meter associated with a four-channel sensor (Skye Instruments, http://www.skyeinstruments.com/), which measures PAR (400–700 nm) and 10 nm windows in the R (664–674 nm) and FR (725–735 nm) regions. Fruit pigment filters were freshly prepared for each experiment. Pericarp samples were homogenized at a 1:2 w/v ratio of tissue (fresh weight) to cold extraction solvent (hexane/acetone/methanol, 2:1:1) using a stainless steel blender. The homogenate was incubated in the dark at 4°C with agitation (320 rpm) for 2 h, and then centrifuged at 5000 ***g*** for 30 min at 4°C. The organic phase enriched in chlorophylls and carotenoids was recovered and directly transferred to glass plates to create the filters (Figure S6). When required, pigment concentration was adjusted by adding extraction solvent to the extracts in the plate until the PAR value of the light passing through the filters was approximately 40–50 μmol m^{-2} sec^{-1}.

Biophotonics

The quantity (transmittance) and quality (R/FR ratio) of white light (400–800 nm) filtered through pericarp sections of tomato fruit was determined using a Lambda 950 UV/VIS/NIR spectrophotometer (Perkin-Elmer, http://www.perkinelmer.com/). Data were sequentially acquired after removing successive layers (200 μm thick) of inner pericarp tissue using a VT12000 S vibrating-blade microtome (Leica, http://www.leika.com/).

Metabolite analysis

Chlorophylls and carotenoids were purified from 15 mg lyophilized tomato pericarp tissue using 1 ml cold extraction solvent as described previously (Saladie *et al.*, 2014), and profiled by HPLC using an Agilent 1200 series HPLC system (Agilent Technologies, http://www.agilent.com) as described previously (Fraser *et al.*, 2000). Absorbance spectra were measured using a quartz cuvette and a SpectraMax M3 multi-mode microplate reader (Molecular Devices, http://www.moleculardevices.com/).

Gene expression analysis

RNA was isolated using PureLink™ RNA Mini and TRIzol Kit (Life Technologies, https://www.thermofisher.com/) and TRIzol (Invitrogen, https://www.thermofisher.com/) according to the manufacturer's instructions, quantified using a NanoDrop 1000 spectrophotometer (Thermo Scientific, http://www.nanodrop.com/), and checked for integrity by agarose gel electrophoresis. A first-strand cDNA synthesis kit (Roche, http://www.roche.com/) was used to generate cDNA according to the manufacturer's instructions. Relative mRNA abundance was evaluated via quantitative PCR using LightCycler 480 SYBR Green I Master Mix (Roche) on a LightCycler 480 real-time PCR system (Roche). At least two technical replicates of each biological replicate were performed, and the mean values were used for further calculations. Normalized transcript abundances were calculated as described previously (Simon, 2003) using tomato *ACT* (Solyc04g011500.2.1) and Arabidopsis *UBC* (At5g25760) as endogenous reference genes. Gene accession numbers and primers used are listed in Table S1.

Phylogenetic analysis

Arabidopsis PIF sequences (Leivar and Quail, 2011) were used as queries to search for putative tomato homologs using BLAST on the National Center for Biotechnology Information website (www.ncbi.nlm.nih.gov/) and the SolGenomics Network website (http://solgenomics.net/). Alignments were performed using MUSCLE (Edgar, 2004a,b) and an unrooted tree was constructed using MEGA5 (Tamura *et al.*, 2011) as described previously (Hall, 2013). Evolutionary relationships were inferred by using the maximum-likelihood method based on the JTT matrix-based model (Jones *et al.*, 1992). The tree with the highest log likelihood (−5298.8282) was selected. Initial tree(s) for the heuristic search were obtained automatically by applying the Neighbor-Joining (NJ) and BioNJ algorithms to a matrix of pairwise distances estimated using a JTT model, and then selecting the topology with superior log likelihood value. A discrete gamma distribution was used to model evolutionary rate differences among sites (five categories (+G, parameter = 0.9307)). The analysis involved 13 amino acid sequences. All positions with less than 95% site coverage were eliminated. A total of 215 positions remained in the final dataset. Analyzed proteins are described in Table S2.

Constructs and plant transformation

Full-length cDNAs encoding PIF1a were amplified from RR fruit and cloned into pDONR207 using Gateway technology (Invitrogen). The sequence was then sub-cloned into pGWB405 (Nakagawa *et al.*, 2007) and into a version of pCAMBIA1301 (Hajdukiewicz *et al.*, 1994) modified for Gateway-compatible cloning using the Gateway vector conversion system (Life Technologies). The pCAMBIA1301-PIF1a construct (35S:PIF1a) was used for *Agrobacterium tumefaciens*-mediated transformation (Bechtold and Pelletier, 1998) of the Arabidopsis *pifq* mutant (Leivar *et al.*, 2009). The pGWB405-PIF1a construct (35S:PIF1a–GFP) was used for transient expression in *N. benthamiana* leaves (Sparkes *et al.*, 2006) and tomato fruit (Orzaez *et al.*, 2006). For VIGS, a 180 bp fragment of the *PIF1a* cDNA was PCR-amplified and cloned into pDONR207 prior to sub-cloning into pTRV2/DR/Gateway (Orzaez *et al.*, 2009). The fragment was designed to minimize off-target silencing. Fruit VIGS was performed as described previously (Orzaez *et al.*, 2009; Fantini *et al.*, 2013). An artificial microRNA (amiRNA) was designed as described previously (Ossowski *et al.*, 2008) to specifically silence *PIF1a* in stably transformed tomato lines. Briefly, plasmid pRS300 was used as template to introduce an anti-*PIF1a* amiRNA sequence into the *miR319a* precursor by site-directed mutagenesis (Schwab *et al.*, 2006). The overlapping PCR amplification steps were performed as described previously (Fernandez *et al.*, 2009), with the exception that primers A and B were re-designed (primers miR A and miR B in Table S3). The resulting PCR product was cloned into pDONR221P4r-P3r to generate plasmid pEF4r-PIF1a-3r. Then plasmids pEF1-2x35S-4, pEF4r-PIF1a-3r and pEF3-Tnos-2 were recombined (Estornell *et al.*, 2009), and the resulted triple recombination was sub-cloned into binary vector pKGW (Karimi *et al.*, 2005) to obtain plasmid pKGW-PIF1a. Tomato MicroTom plants were transformed with pKGW-PIF1a as previously described (Fernandez *et al.*, 2009). All constructs were confirmed by restriction mapping and DNA sequence analysis. Primers are listed in Table S3.

Confocal microscopy

After agroinfiltration of *N. benthamiana* leaves with pGWB405-PIF1a as described previously (Sparkes *et al.*, 2006), PIF1a–GFP fluorescence was detected using a Leica TCS SP5 confocal laser-scanning microscope. Nuclei were identified by directly incubating the leaf samples with 4′,6–diamidino-2–phenylindole (DAPI) (1 mg ml^{-1}). Excitation filters of 450–490 nm and 410–420 nm were used for detection of GFP fluorescence and DAPI signal, respectively. PIF1a–GFP levels in individual nuclei were estimated by quantifying the GFP fluorescence signal in *z*–stacks of optical sections separated by 0.5 μm using the integrated microscope software. To estimate PIF1a–GFP stability in response to light, GFP fluorescence in the nuclei found in a given field was quantified in the dim light of the microscope room and then the microscope stage was moved down to expose the sample to either R (30 μmol m^{-2} sec^{-1}) or FR (30 μmol m^{-2} sec^{-1}) using a portable QBEAM 2200 LED lamp (Quantum Devices, http://www.quantum-dev.com/). After illumination for 5 min, the microscope stage was moved up to quantify the GFP signals in the same field. GFP excitation was limited to image acquisition steps to minimize photobleaching. Control samples were treated similarly except that they were not irradiated. Tomato pericarp sections were obtained using a Vibratome series 1000 sectioning system (Vibratome, http://www.vibratome.com/). Chloroplasts were identified using excitation at 488 nm and a 610–700 nm filter to detect chlorophyll autofluorescence.

ChIP analysis

Tomato Moneymaker fruit at the MG stage were agroinjected with pGWB405-PIF1a as described previously (Orzaez *et al.*, 2006) to produce the PIF1a–GFP protein. GFP fluorescence in pericarp sections was monitored using a Blak-Ray B–100AP high-intensity UV lamp (Ultra-Violet Products, http://www.uvp.com/). Pericarp sections showing fluorescence were then excised using a scalpel, fixed with 1% formaldehyde for 15 min under vacuum, and then ground to fine powder under liquid nitrogen. ChIP assays were performed as described previously (Osnato *et al.*, 2012) using a commercial anti-GFP antibody (Life Technologies). An anti-HA antibody (Santa Cruz Biotechnology, http://www.scbt.com/) was used in parallel control reactions. Primers for quantitative PCR reactions are listed in Table S4.

Statistical analysis

Student's *t* test, ANOVA followed by the Newman–Keuls multiple comparison post hoc test and Pearson correlation coefficients (*r* values) were calculated using GraphPad Prism 5.0a (GraphPad Software, http://www.graphpad.com/).

ACCESSION NUMBERS

Accession numbers for genes analyzed by quantitative RT–PCR and for protein sequences used for molecular phylogenetic analysis are listed in Tables S1 and S2, respectively.

ACKNOWLEDGMENTS

We thank Cathie Martin (Department of Metabolic Biology, John Innes Centre, Norwich Research Park, Norwich NR4 7UH, UK) and José Luis Riechmann for critical reading of the manuscript, Jaime F. Martínez-García for valuable discussion, and César Alonso-Ortega for providing some of the equipment used in this work. We gratefully acknowledge the experimental advice of Luis Matías-Hernández and technical assistance of María Rosa Rodríguez-Goberna and core facilities staff of the Centre for Research in Agricultural Genomics. Work at the Centre for Research in Agricultural Genomics was funded by the following grants: CarotenActors (FP7-PEOPLE-2011-IIF 300862), TiMet

(FP7-KBBE-2009-3 245143), Ibercarot (CYTED-112RT0445), Spanish Ministerio de Economia y Competitividad (BIO2011-23680) and Generalitat de Catalunya (2014SGR-1434) to MRC. Work by researchers at the Institut de Ciencies Fotoniques was partially performed at the super-resolution light nanoscopy facility and supported by Fundació Cellex Barcelona.

SUPPORTING INFORMATION

Additional Supporting Information may be found in the online version of this article.

Figure S1. Tomato fruit ripening stages and photosynthetic pigment composition.

Figure S2. *PSY1* response to R and FR.

Figure S3. Specificity of the amiRNA against PIF1a.

Figure S4. Light spectra at various depths of the pericarp.

Figure S5. R/FR ratio of sunlight filtered through the pericarp of tomato fruit.

Figure S6. Set-up for experiments with tomato fruit pigment extracts.

Figure S7. Effect of light filtered through tomato fruit pigment extracts on Arabidopsis shade-responsive gene expression.

Table S1. Accession IDs and primers for genes analyzed by quantitaive RT–PCR.

Table S2. Accession IDs for protein sequences used for molecular phylogenetic analysis.

Table S3. Primers used in cloning.

Table S4. Primers used for ChIP/quantitative PCR analysis.

REFERENCES

Alba, R., Cordonnier-Pratt, M.M. and Pratt, L.H. (2000) Fruit-localized phytochromes regulate lycopene accumulation independently of ethylene production in tomato. *Plant Physiol.* **123**, 363–370.

Al–Sady, B., Ni, W., Kircher, S., Schafer, E. and Quail, P.H. (2006) Photoactivated phytochrome induces rapid PIF3 phosphorylation prior to proteasome-mediated degradation. *Mol. Cell*, **23**, 439–446.

Azari, R., Reuveni, M., Evenor, D., Nahon, S., Shlomo, H., Chen, L. and Levin, I. (2010) Overexpression of UV-DAMAGED DNA BINDING PROTEIN 1 links plant development and phytonutrient accumulation in *high pigment–1* tomato. *J. Exp. Bot.* **61**, 3627–3637.

Bae, G. and Choi, G. (2008) Decoding of light signals by plant phytochromes and their interacting proteins. *Annu. Rev. Plant Biol.* **59**, 281–311.

Bechtold, N. and Pelletier, G. (1998) *In planta Agrobacterium*-mediated transformation of adult *Arabidopsis thaliana* plants by vacuum infiltration. *Methods Mol. Biol.* **82**, 259–266.

Bou-Torrent, J., Toledo-Ortiz, G., Ortiz-Alcaide, M., Cifuentes-Esquivel, N., Halliday, K.J., Martinez-Garcia, J.F. and Rodriguez-Concepcion, M. (2015) Regulation of carotenoid biosynthesis by shade relies on specific subsets of antagonistic transcription factors and co-factors. *Plant Physiol.* **169**, 1584–1594.

Casal, J.J. (2013) Photoreceptor signaling networks in plant responses to shade. *Annu. Rev. Plant Biol.* **64**, 403–427.

Cheung, A.Y., McNellis, T. and Piekos, B. (1993) Maintenance of chloroplast components during chromoplast differentiation in the tomato mutant green flesh. *Plant Physiol.* **101**, 1223–1229.

Edgar, R.C. (2004a) MUSCLE: a multiple sequence alignment method with reduced time and space complexity. *BMC Bioinformatics*, **5**, 113.

Edgar, R.C. (2004b) MUSCLE: multiple sequence alignment with high accuracy and high throughput. *Nucleic Acids Res.* **32**, 1792–1797.

Estornell, L.H., Orzaez, D., Lopez-Pena, L., Pineda, B., Anton, M.T., Moreno, V. and Granell, A. (2009) A multisite Gateway-based toolkit for targeted gene expression and hairpin RNA silencing in tomato fruits. *Plant Biotechnol. J.* **7**, 298–309.

Fantini, E., Falcone, G., Frusciante, S., Giliberto, L. and Giuliano, G. (2013) Dissection of tomato lycopene biosynthesis through virus-induced gene silencing. *Plant Physiol.* **163**, 986–998.

Fernandez, A.I., Viron, N., Alhagdow, M. *et al.* (2009) Flexible tools for gene expression and silencing in tomato. *Plant Physiol.* **151**, 1729–1740.

Fraser, P.D. and Bramley, P.M. (2004) The biosynthesis and nutritional uses of carotenoids. *Prog. Lipid Res.* **43**, 228–265.

Fraser, P.D., Pinto, M.E., Holloway, D.E. and Bramley, P.M. (2000) Application of high-performance liquid chromatography with photodiode array detection to the metabolic profiling of plant isoprenoids. *Plant J.* **24**, 551–558.

Fraser, P.D., Romer, S., Shipton, C.A., Mills, P.B., Kiano, J.W., Misawa, N., Drake, R.G., Schuch, W. and Bramley, P.M. (2002) Evaluation of transgenic tomato plants expressing an additional phytoene synthase in a fruit-specific manner. *Proc. Natl Acad. Sci. USA*, **99**, 1092–1097.

Fray, R.G. and Grierson, D. (1993) Identification and genetic analysis of normal and mutant phytoene synthase genes of tomato by sequencing, complementation and co-suppression. *Plant Mol. Biol.* **22**, 589–602.

Fujisawa, M., Nakano, T., Shima, Y. and Ito, Y. (2013) A large-scale identification of direct targets of the tomato MADS box transcription factor RIPENING INHIBITOR reveals the regulation of fruit ripening. *Plant Cell*, **25**, 371–386.

Fujisawa, M., Shima, Y., Nakagawa, H., Kitagawa, M., Kimbara, J., Nakano, T., Kasumi, T. and Ito, Y. (2014) Transcriptional regulation of fruit ripening by tomato FRUITFULL homologs and associated MADS box proteins. *Plant Cell*, **26**, 89–101.

Giorio, G., Stigliani, A.L. and D'Ambrosio, C. (2008) Phytoene synthase genes in tomato (*Solanum lycopersicum* L.) – new data on the structures, the deduced amino acid sequences and the expression patterns. *FEBS J.* **275**, 527–535.

Gupta, S.K., Sharma, S., Santisree, P., Kilambi, H.V., Appenroth, K., Sreelakshmi, Y. and Sharma, R. (2014) Complex and shifting interactions of phytochromes regulate fruit development in tomato. *Plant, Cell Environ.* **37**, 1688–1702.

Hajdukiewicz, P., Svab, Z. and Maliga, P. (1994) The small, versatile pPZP family of *Agrobacterium* binary vectors for plant transformation. *Plant Mol. Biol.* **25**, 989–994.

Hall, B.G. (2013) Building phylogenetic trees from molecular data with MEGA. *Mol. Biol. Evol.* **30**, 1229–1235.

Jones, D.T., Taylor, W.R. and Thornton, J.M. (1992) The rapid generation of mutation data matrices from protein sequences. *Comput. Appl. Biosci.* **8**, 275–282.

Karimi, M., De Meyer, B. and Hilson, P. (2005) Modular cloning in plant cells. *Trends Plant Sci.* **10**, 103–105.

Klee, H.J. and Giovannoni, J.J. (2011) Genetics and control of tomato fruit ripening and quality attributes. *Annu. Rev. Genet.* **45**, 41–59.

Ku, H., Vision, T., Liu, J., and Tranksley, S.D. (2000) Comparing sequenced segments of the tomato and Arabidopsis genomes: Large-scale duplication followed by selective gene loss creates a network of synteny. *Proc. Natl Acad. Sci. USA*, **97**, 9121–9126.

Leivar, P. and Monte, E. (2014) PIFs: systems integrators in plant development. *Plant Cell*, **26**, 56–78.

Leivar, P. and Quail, P.H. (2011) PIFs: pivotal components in a cellular signaling hub. *Trends Plant Sci.* **16**, 19–28.

Leivar, P., Tepperman, J.M., Monte, E., Calderon, R.H., Liu, T.L. and Quail, P.H. (2009) Definition of early transcriptional circuitry involved in light-induced reversal of PIF-imposed repression of photomorphogenesis in young *Arabidopsis* seedlings. *Plant Cell*, **21**, 3535–3553.

Liu, Y., Roof, S., Ye, Z., Barry, C., van Tuinen, A., Vrebalov, J., Bowler, C. and Giovannoni, J. (2004) Manipulation of light signal transduction as a means of modifying fruit nutritional quality in tomato. *Proc. Natl Acad. Sci. USA*, **101**, 9897–9902.

Martel, C., Vrebalov, J., Tafelmeyer, P. and Giovannoni, J.J. (2011) The tomato MADS-box transcription factor RIPENING INHIBITOR interacts with promoters involved in numerous ripening processes in a COLORLESS NONRIPENING-dependent manner. *Plant Physiol.* **157**, 1568–1579.

Martínez-García, J.F., Galstyan, A., Salla-Martret, M., Cifuentes-Esquivel, N., Gallemí, M. and Bou-Torrent, J. (2010) Regulatory components of shade avoidance syndrome. *Adv. Bot. Res.* **53**, 65–116.

Nakagawa, T., Suzuki, T., Murata, S. *et al.* (2007) Improved Gateway binary vectors: high-performance vectors for creation of fusion constructs in transgenic analysis of plants. *Biosci. Biotechnol. Biochem.* **71**, 2095–2100.

Neff, M.M., Fankhauser, C. and Chory, J. (2000) Light: an indicator of time and place. *Genes Dev.* **14**, 257–271.

Orzaez, D., Mirabel, S., Wieland, W.H. and Granell, A. (2006) Agroinjection of tomato fruits. A tool for rapid functional analysis of transgenes directly in fruit. *Plant Physiol.* **140**, 3–11.

Orzaez, D., Medina, A., Torre, S., Fernandez-Moreno, J.P., Rambla, J.L., Fernandez-Del-Carmen, A., Butelli, E., Martin, C. and Granell, A. (2009) A visual reporter system for virus-induced gene silencing in tomato fruit based on anthocyanin accumulation. *Plant Physiol.* **150**, 1122–1134.

Osnato, M., Castillejo, C., Matias-Hernandez, L. and Pelaz, S. (2012) TEMPRANILLO genes link photoperiod and gibberellin pathways to control flowering in *Arabidopsis*. *Nat. Commun.* **3**, 808.

Ossowski, S., Schwab, R. and Weigel, D. (2008) Gene silencing in plants using artificial microRNAs and other small RNAs. *Plant J.* **53**, 674–690.

Ruiz-Sola, M.A. and Rodriguez-Concepcion, M. (2012) Carotenoid biosynthesis in Arabidopsis: a colorful pathway. *Arabidopsis Book*, **10**, e0158.

Ruiz-Sola, M.A., Arbona, V., Gomez-Cadenas, A., Rodriguez-Concepcion, M. and Rodriguez-Villalon, A. (2014a) A root specific induction of carotenoid biosynthesis contributes to ABA production upon salt stress in arabidopsis. *PLoS ONE*, **9**, e90765.

Ruiz-Sola, M.A., Rodriguez-Villalon, A. and Rodriguez-Concepcion, M. (2014b) Light-sensitive phytochrome-interacting factors (PIFs) are not required to regulate phytoene synthase gene expression in the root. *Plant Signal Behav.* **9**, e29248.

Saladie, M., Wright, L.P., Garcia-Mas, J., Rodriguez-Concepcion, M. and Phillips, M.A. (2014) The 2-C-methylerythritol 4-phosphate pathway in melon is regulated by specialized isoforms for the first and last steps. *J. Exp. Bot.* **65**, 5077–5092.

Schofield, A. and Paliyath, G. (2005) Modulation of carotenoid biosynthesis during tomato fruit ripening through phytochrome regulation of phytoene synthase activity. *Plant Physiol. Biochem.* **43**, 1052–1060.

Schwab, R., Ossowski, S., Riester, M., Warthmann, N. and Weigel, D. (2006) Highly specific gene silencing by artificial microRNAs in *Arabidopsis*. *Plant Cell*, **18**, 1121–1133.

Seymour, G.B., Ostergaard, L., Chapman, N.H., Knapp, S. and Martin, C. (2013) Fruit development and ripening. *Annu. Rev. Plant Biol.* **64**, 219–241.

Shen, H., Zhu, L., Castillon, A., Majee, M., Downie, B. and Huq, E. (2008) Light-induced phosphorylation and degradation of the negative regulator PHYTOCHROME-INTERACTING FACTOR1 from *Arabidopsis* depend upon its direct physical interactions with photoactivated phytochromes. *Plant Cell*, **20**, 1586–1602.

Shima, Y., Kitagawa, M., Fujisawa, M., Nakano, T., Kato, H., Kimbara, J., Kasumi, T. and Ito, Y. (2013) Tomato FRUITFULL homologues act in fruit ripening via forming MADS-box transcription factor complexes with RIN. *Plant Mol. Biol.* **82**, 427–438.

Shin, J., Kim, K., Kang, H., Zulfugarov, I.S., Bae, G., Lee, C.H., Lee, D. and Choi, G. (2009) Phytochromes promote seedling light responses by inhibiting four negatively-acting phytochrome-interacting factors. *Proc. Natl Acad. Sci. USA*, **106**, 7660–7665.

Simon, P. (2003) Q-Gene: processing quantitative real-time RT–PCR data. *Bioinformatics*, **19**, 1439–1440.

Sorin, C., Salla-Martret, M., Bou-Torrent, J., Roig-Villanova, I. and Martinez-Garcia, J.F. (2009) ATHB4, a regulator of shade avoidance, modulates hormone response in Arabidopsis seedlings. *Plant J.* **59**, 266–277.

Sparkes, I.A., Runions, J., Kearns, A. and Hawes, C. (2006) Rapid, transient expression of fluorescent fusion proteins in tobacco plants and generation of stably transformed plants. *Nat. Protoc.* **1**, 2019–2025.

Tamura, K., Peterson, D., Peterson, N., Stecher, G., Nei, M. and Kumar, S. (2011) MEGA5: molecular evolutionary genetics analysis using maximum likelihood, evolutionary distance, and maximum parsimony methods. *Mol. Biol. Evol.* **28**, 2731–2739.

Toledo-Ortiz, G., Huq, E. and Quail, P.H. (2003) The Arabidopsis basic/helix-loop-helix transcription factor family. *Plant Cell*, **15**, 1749–1770.

Toledo-Ortiz, G., Huq, E. and Rodriguez-Concepcion, M. (2010) Direct regulation of phytoene synthase gene expression and carotenoid biosynthesis by phytochrome-interacting factors. *Proc. Natl Acad. Sci. USA*, **107**, 11626–11631.

Toledo-Ortiz, G., Johansson, H., Lee, K.P., Bou-Torrent, J., Stewart, K., Steel, G., Rodriguez-Concepcion, M. and Halliday, K.J. (2014) The HY5-PIF regulatory module coordinates light and temperature control of photosynthetic gene transcription. *PLoS Genet.* **10**, e1004416.

Tomato Genome Consortium. (2012) The tomato genome sequence provides insights into fleshy fruit evolution. *Nature*, **485**, 635–641.

Trupkin, S.A., Legris, M., Buchovsky, A.S., Tolava Rivero, M.B. and Casal, J.J. (2014) Phytochrome B nuclear bodies respond to the low red to far-red ratio and to the reduced irradiance of canopy shade in Arabidopsis. *Plant Physiol.* **165**, 1698–1708.

Zhang, Y., Mayba, O., Pfeiffer, A., Shi, H., Tepperman, J.M., Speed, T.P. and Quail, P.H. (2013) A quartet of PIF bHLH factors provides a transcriptionally centered signaling hub that regulates seedling morphogenesis through differential expression-patterning of shared target genes in *Arabidopsis*. *PLoS Genet.* **9**, e1003244.

Zhong, S., Fei, Z., Chen, Y.R. *et al.* (2013) Single-base resolution methylomes of tomato fruit development reveal epigenome modifications associated with ripening. *Nat. Biotechnol.* **31**, 154–159.

